IJCTA, 10(03), 2017, pp. 265-275

Effects of Staff Movement and Air Change Rate on the Airflow Fields in a Hospital's Operating Room

Keng Yinn Wong* Haslinda Mohamed Kamar* Nazri Kamsah* and Fazila Mohd. Zawawi*

Abstract : Airborne particles in operating rooms (OR) are strongly related to an increased risk of surgical site infection. The particles level is commonly minimised using cleanroom-derived airflow systems. This study investigates the effects of hospital staff displacement and air change rate per hour (ACH) on airflow fields inside an OR. A simplified three-dimensional model of the OR was developed using the Computational Fluid Dynamics software. A flow model using SST k-ω model based on the Reynolds-Averaged Navier-Stokes (RANS) equations was carried out to predict the distribution of air velocity. Staff lateral motion was simulated by pre-defined dynamic meshes using a user-defined function (UDF). A parametric study was carried out to examine the effects of human movement and ACH on the air velocity distribution inside the OR. Results show that lateral human movement created a significant effect on the airflow patterns inside the OR. However, there is no impact for the case of ACH. As the travelling speed of the staff increases to 1.5 m/s, the higher air velocity region developed in the vicinity of the back area of the personnel.

Keywords : Operating room; CFD simulation; dynamic mesh; user-defined function; air change rate.

1. INTRODUCTION

A hospital's operating room (OR) is the main healthcare facility used to perform surgical procedures. The majority of ORs worldwide employ the cleanroom technology to provide a highly controlled and clean environment for both the patients and the hospital's personnel. However, in recent studies, they concluded that a high surgical site infection (SSI) rate was due to a higher level of airborne particles at the surgical sites [1]. Among others are a study done by Karlatti and Hannavar [2], where they found that the post-operational SSI rates were increasing when the surgery was performed in unclean surroundings. It was estimated that nearly 3% to 5% of the patients who underwent surgery in clean environments developed SSIs [3],whereas surgical procedures performed in ultraclean environments were associated with an SSI incidence rate as low as 1% [4].The application of a proper ventilation system inside those controlled environments could reduce numbers of SSI [5].

An SSI is defined as any infection that follows an operative procedure and occurs at or near the surgical incision within 30 days of the procedure [2, 6]. SSIs are ranked third amongst the most common Healthcare-Associated Infections (HAI). They make up nearly 13-17% [5, 7] and 10-40% [3] of the total HAI cases reported in Europe and the US, respectively. Singh et al. [3] found out that in over 27 million operations performed annually in the US, SSIs were reported in approximately 300,000 cases, of which 8,000 ended up in fatalities [3]. SSIs are associated with an increased risk of death, additional treatment costs and prolong hospital stays. The rate of post-operative morbidity has increased by 65 to 80% due to the increment of the number of SSI [8] and has caused the rise of hospitalisation costs by 3-29 thousand US dollars per case depending on the type of the surgical procedure performed [9]. One of the valid

* Faculty of Mechanical Engineering, Universiti Teknologi Malaysia, 81310 UTM Skudai, Johor, Malaysia.

examples is a case study presented by Chow and Wang in 2012, where the medical care expenses for a patient with a prosthetic joint SSI has reached to $100,000 US due to longer stay in the hospital by up to 7-10 days on average [9, 10].

The ventilation system inside an OR is specially designed to produce a free particle sediments environment. The principal use of this system is to filter the unwanted residues from the outdoor to enter the room and to remove the existing particles to the adjacent area. The direction of the airflow and the rate of air-change (ACH) in the OR are the main factors in determining the amount of airborne particle settlement [11, 32]. ACH is defined as the measure of the supply air volume added to a confined space in an hour. Under an adequate air exchange condition, the contaminated air could effectively replace by the fresh-clean air. A The American Society of Heating, Refrigerating, and Air-Conditioning Engineers (ASHRAE) [12] recommended practitioners to employ a unidirectional airflow ventilation in the OR. The supply air is located at the ceiling, while the exhaust air is removed to the adjacent area by exhaust grilles near the floor. The unidirectional airflow is capable of reducing the number of airborne bacteria and the risk of surface contamination at the surgical sites [13]. A proper ACH could add a further improvement in reducing particles amount inside the OR. Many studies have been carried out to ascertain the appropriate ACH, the proposed ACH is in the range of 8/h to 20/h[14-16]. For a constant particle generation rate inside an OR, the higher ACH could improve the removal rates of the airborne particles.

This article presents results of a study on the effects of moving surgical staff and ACH rates on the distribution of air velocity inside an operating room (OR). A computational fluid dynamics (CFD) method was used to develop a simplified model of the OR. An SST k-ω model based on the Reynolds-Averaged Navier-Stokes (RANS) equations was carried out to predict the distribution of air velocity. A parametric study was performed to examine the influences of human movement and ACH on the air velocity distribution inside the OR. Three moving speeds of the staff and ACHs were considered. The considered staff moving rates are 0.5, 1.0 and 1.5 m/s, while the ACHs are 41/h, 52/h and 63/h.

2. METHODOLOGY

2.1. Case Study

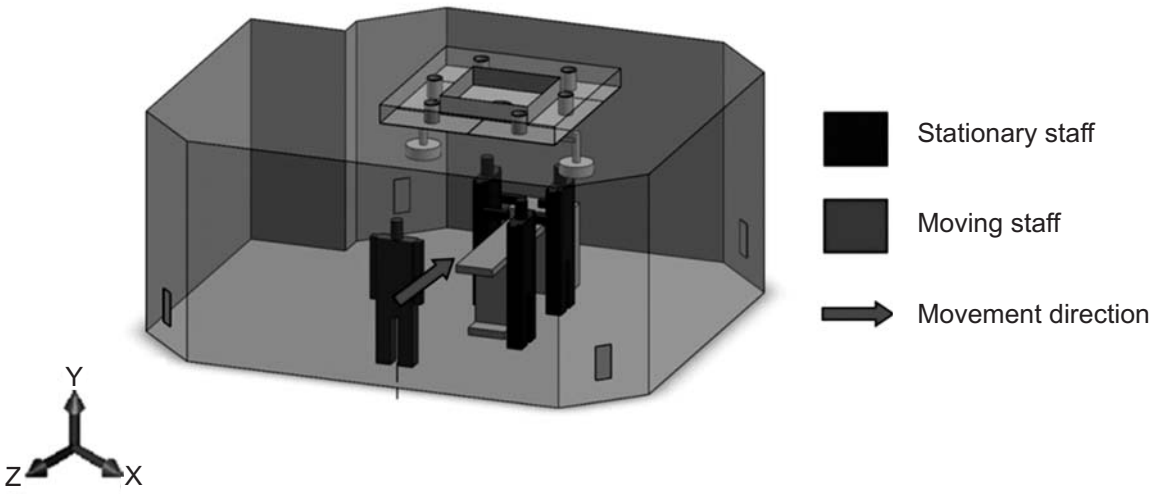

Figure 1: Simplified CFD model of the operating room with three surgery staffs in an upright standing posture (blue) and one staff is moving towards the operating table (red)

The tested operating room is based on the actual operating room of a private hospital located in Malaysia. The air is supplied into the room through the supply air diffusers mounted at the ceiling. The air filtration for the operating room is carried out in three stages. The first and second stage filters have a trapping efficiency of 30% and 95%, respectively. The third stage, known as a high-efficiency particulate air (HEPA) filter is capable of trapping 99.97% of particles with sizes larger than 0.3 μm. About 10% of the

total ceiling area is covered by the supply air diffuser and surgical lamp fixtures. The operating room has a positive pressurization. The air is exhausted through exhaust grilles located at the four corners of the lower section of the operating room walls. The supply air diffuser covers the entire perimeter of the operating table. A total of four medical staffs were placed around an operating table. A lateral displacement with three different speeds was prescribed at one personnel, *i.e*. 0.5, 1.0 and 1.5 m/s. These speeds have been reported as the human walking speed in healthcare facilities [17]. Zero velocity was specified at the remainder staffs. As illustrated in Figure 1, the moving staff is coloured in red travels along the z-axis towards the surgical table.

Three different ACH rates were examined: 41/h, 52/h and 63/h. These ACH values are obtained by changing the supply air velocity as recommended by IEST standard [18], *i*.e. 0.36 m/s, 0.45 m/s, and 0.54 m/s. Equation (1) expresses the ACH for a positive pressure operating room [19]. The flow model was performed under transient conditions.

$$\text{Air Change Rate per Hour} = \frac{\text{Supply Air Velocity}\left(\frac{\text{m}}{\text{min}}\right) \times \text{Supply Air Area (m}^2\text{)} \times 60}{\text{Room Volume (m}^3\text{)}} \quad (1)$$

2.2 Description of CFD Model

Figure 2 shows a simplified CFD model of the hospital operating room. The model includes an operating table, supply air diffusers and air exhaust grilles. The supply air diffusers measure 1.2 m (W) × 0.6 m (L) while the exhaust air grilles have the dimension of 0.22 m (W) × 0.46 m (L). There is a total of six air supply diffusers located at the ceiling of the operating room, directly above the operating table. They were designed such that the downward air flow covers the entire area of the operating table with a 305 mm offset on all sides of the table. This feature is to fulfil the requirement of the ASHRAE Standard 170 [20]. Each exhaust grille has an active area of 0.084 m^2. They are located in the middle of the four sides of the room wall, at a height of 0.25 m from the floor.

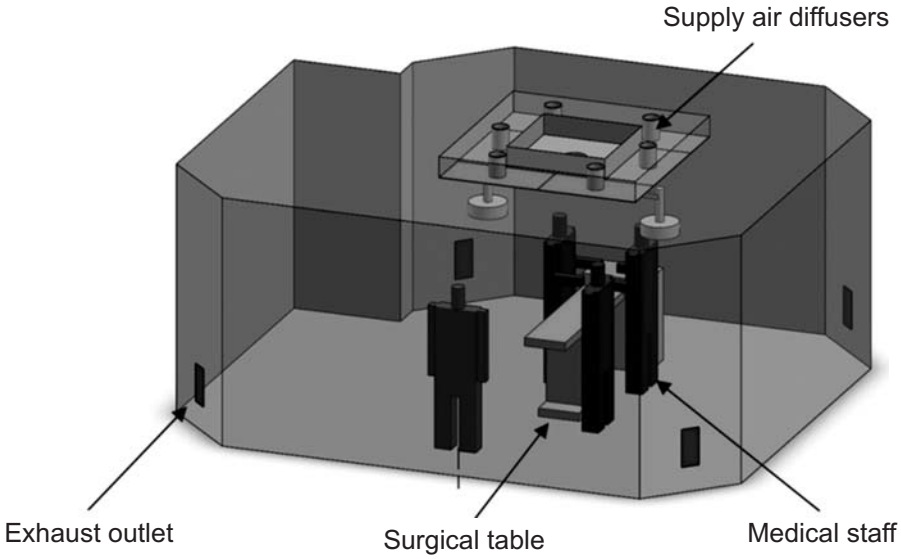

Figure 2: Major components of the simplified CFD model of the operating room

2.3. Meshing of Computational Domain

The ANSYS CFD software was used to mesh the computational domain of the CFD model. The model was discretized with an unstructured mesh composed of tetrahedral elements. A growth rate of 1.20 was used between the mesh layers to obtain a reliable prediction of wall boundary layers. Mesh refinement was applied in areas where a significant variation of airflow field occurred [21] *i.e*., the surfaces of the medical

personnel, supply air diffusers, return air grilles, surgical table and two surgical lamps. Element surface size ranged between 4.8×10^{-3} and 0.25 m; and the maximum skewness is 0.81.

Grid independence test (GIT) was carried out to establish the number of elements that would minimise the effects of meshing on the results of the simulations. Selecting fewer elements could lead to a poor discretization, while too many could lengthen the simulation time. Four sets of element numbers were tested, namely from 1,000,000 up to 7,000,000 elements. The variation of airflow velocity along the *z*-axis at 1.2 m above the floor level in the model for a different number of elements is plotted, as shown in Figure 3. It can be seen that the airflow velocity is nearly unchanged when 2,500,000 elements were used to mesh the computational domain.

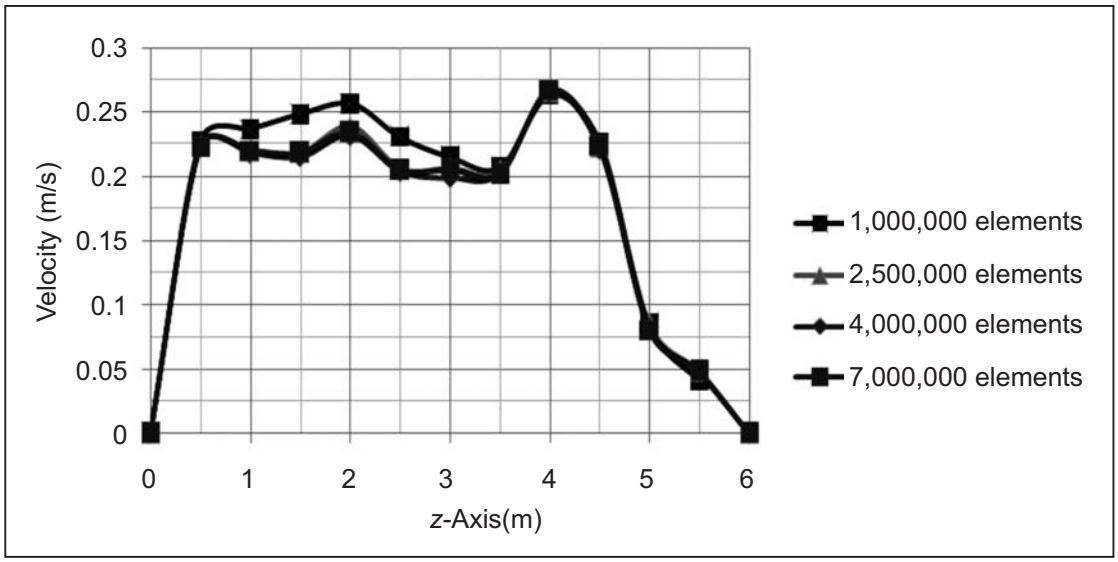

Figure 3: The airflow velocity variation on a plane of 1.2 m height from the floor for a different number of elements

2.4. Prescription of Boundary Conditions

Table 1

Boundary conditions prescribed in the CFD model

Zone	*Type*	*Boundary conditions*
Surgical table	Wall	• Wall motion: Stationary wall • Shear condition: No slip
Floor	Wall	• Wall motion: Stationary wall
Static staff	Wall	• Type: Wall
Moving staff	Wall	• Wall condition: Stationary wall
Supply air diffusers	Velocity inlet	• Velocity specification method - magnitude: Normal to boundary 0.36 m/s (ACH = 41/h) 0.45 m/s (ACH = 52/h) 0.54 m/s (ACH = 63/h) • Temperature: 293 K • Turbulent intensity: 5%
Exhaust outlets	Pressure outlet	• Gauge pressure: 0 Pa

Table 1 lists the boundary conditions prescribed on the CFD model for the flow analysis. Inlet air flow condition was specified at the ceiling mounted diffusers. A no-slip condition applied to the wall boundaries. A UDF code that defined the dynamic movement of the staff was incorporated into the ANSYS Fluent software. The code was generated using Microsoft Visual C++ programming language. All airflow boundary conditions were specified in the direction normal to the respective surfaces. A zero gage pressure condition was set at the exhaust grilles, which serve as the air outlets. The air flow inside the operating room was assumed as incompressible.

2.5. Selection of Airflow Model

The governing equations that describe the fluid flow within an enclosure are all based on the conservation of mass, momentum and energy within the space. Several flow models are available in the CFD software to simulate the airflow inside the computational domain. These are Reynolds-Averaged Navier- Stokes (RANS) family equations which include the *k*-ε, *k*-ω, transition SST, detached eddy simulation (DES) and large eddy simulation (LES) models [22-26]. When compared to all the models above, the RANS model is adequate for solving a transient airflow and giving sufficiently reliable results. While, the applications of DES and LES demand a high computational power and longer computation time [22, 25]. Therefore, in this study, the flow model was examined under a transient condition using the SST *k*-ω RANS model including both SIMPLE [13, 23, 25, 27, 28] and SIMPLEC algorithms [22].

The SST *k*-ω model was shown in previous works to be reliable in producing both near-wall and far-field airflow predictions[29]. The governing equations for the SST k-ω model are given by Equations (2) and (3) below [30]:

$$\partial(\rho k)/\partial t + \partial(\rho k \acute{u}_i)/\partial x_i = \partial(\Gamma k\, \partial k/\partial x_j)/\partial x_j + \hat{G}_k - Y_k + S_k \quad (2)$$

$$\partial(\rho \omega)/\partial \tau + \partial(\rho \omega \acute{u}_i)/\partial x_i = \partial(\Gamma \omega\, \partial \omega/\partial x_j)/\partial x_j + G_\omega - Y_\omega + D_\omega + S_\omega \quad (3)$$

where

ρ = fluid density
t = time
$\acute{u}_i$ = velocity component
x_i = coordinates
μ = fluidviscosity
k = kinetic energy
ω = specific rate of dissipation
Γ = effective diffusion parameter
G = turbulence kinetic energy
Y = dissipation due to turbulence
D = cross-diffusion term
S_i = source term

A SIMPLEC algorithm was selected to handle the coupling effects between the flow velocity and pressure. A QUICK discretization scheme was selected to reduce the effects of numerical diffusion on the solution as it would help improve the accuracy. A convergence criterion of 1×10^{-4} was chosen to ensure a good convergence of the flow analyses. The time interval of 0.001 second was considered for the transient simulations with maximum allowable iterations of 30. The turbulent intensity was set at 5%. A UDF code that defined the dynamic movement of the staff was embedded into the ANSYS Fluent software.

2.6. Air Flow Velocity Validation

The airflow simulation was validated under a steady-state condition. The simulated results were compared with airflow velocities obtained from the field measurement. A CFD model of the operating room was based on the actual operating room of a private hospital located in Malaysia. The CFD model includes an

operating table, supply air diffusers and air exhaust grilles. The model was meshed using the tetrahedral cells with a maximum skewness of 0.81. The minimum and maximum elements sizes are 4.8×10^{-3} and 0.25 m, respectively. An SST *k*-ω turbulence model was used to perform the airflow simulation. An airflow velocity of 0.45 m/s was prescribed at all the supply air diffusers as the boundary conditions, which was based on actual measured data. A zero-gauge pressure boundary condition was specified at all the air outlet grilles. The air flow inside the operating room was assumed as incompressible. A no-slip condition was defined at all the wall surfaces. The second order upwind scheme was used for pressure, momentum, turbulence kinetic energy, and turbulent dissipation rate. A convergence criterion of 1×10^{-4} was selected to ensure a good convergence of the flow analyses.

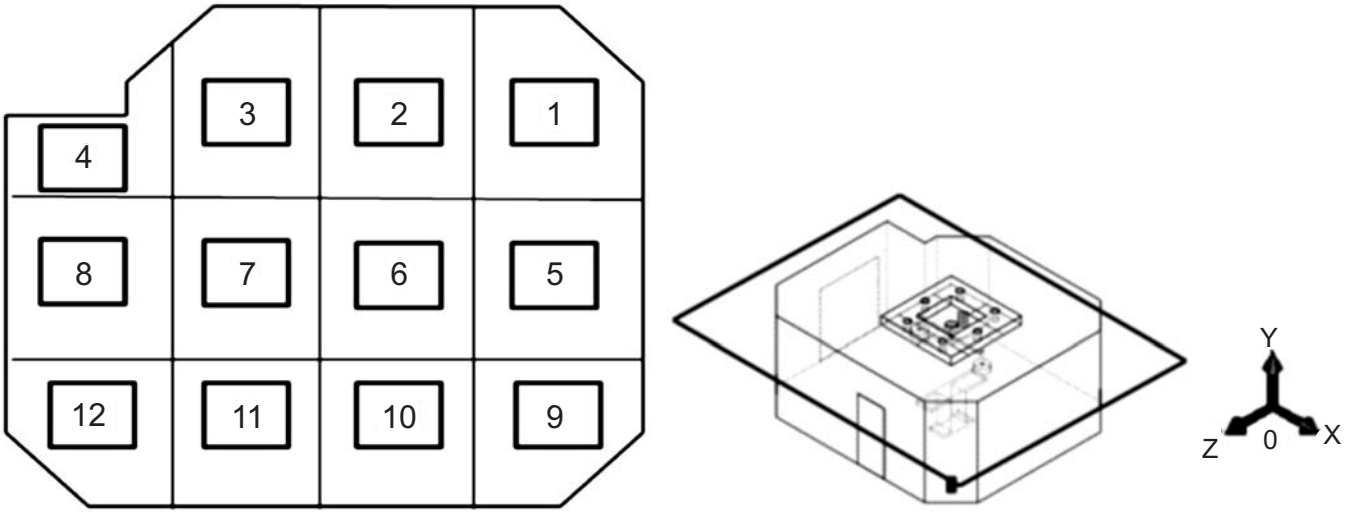

Figure 4: Sampling locations of airflow velocity on a plane of 1.2 m above the floor level

Figure 4 illustrates the measuring points on the horizontal plane at a height of 1.2 m from the floor inside the operating room. The sampling points were established according to IEST standard [18], in which each grid section could not exceed 30 m^2. Figure 5 shows the comparison between simulated results and of the measured airflow velocities at all measuring points. It can be observed from the figure that there is a good agreement between the simulation and the measured results. The difference in the airflow velocities was found to be about 7.8%. This value can be considered acceptable since it is well below 20% [31].

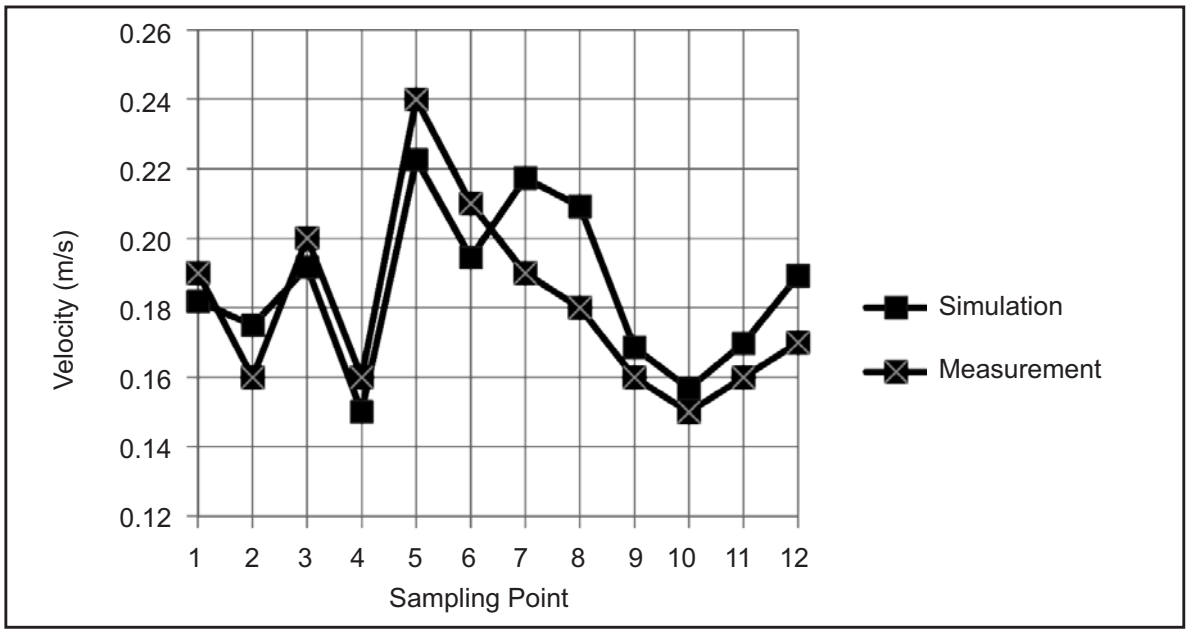

Figure 5: Comparison between the measured and predicted airflow velocity variation on a plane of 1.2 m height from the floor

3. RESULTS AND DISCUSSION

The airflow distribution inside the OR were examined for various values of moving rates of a staff and ACHs of the OR. The results of the parametric analysis are illustrated in Figures 6 through 9. Figures 6 (*a*) – (*f*) show the distributions of the airflow as a staff travels towards the operating table along the *z*-axis at a rate of 0.5 m/s under various ACHs of 41/h, 52/h, and 63/h. It was found that the interference of the moving person into the air stream has developed a higher air velocity zone in the vicinity of the body as compared to the other regions, i.e. around 0.45 m/s. No significant differences can be seen on the airflow pattern when the ACH increases from 41/h to 63/h.

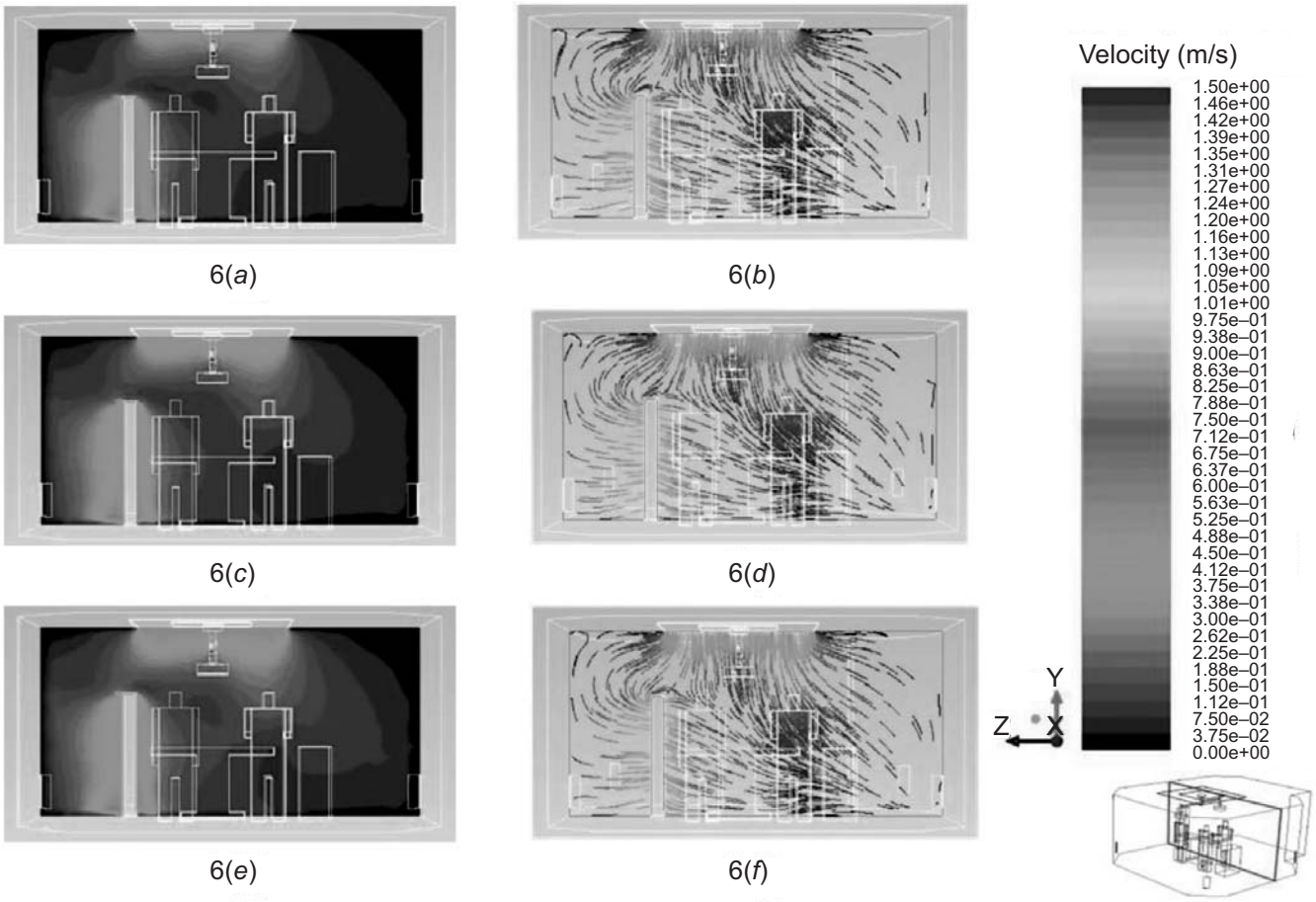

Figure 6: Airflow velocity distributions when a staff travels at a rate of 0.5 m/s under various ACH values of (*a* & *b*) 41/h, (*c* & *d*) 52/h, (*e* & *f*) 63/h

Figures 7(*a*) – (*f*) show the airflow velocity patterns inside the OR when the staff moves towards the operating table at a rate of 1.0 m/s along the *z*-axis under various ACH values. A slightly higher air velocity field has been developed around the body of the moving person when compared to the former case, *i.e*. around 1.05 m/s. A smooth swirling flow pattern can also be noticed in the area near to the head. The average air velocity around the person approaching the operating table increases with the ACH of the room and the staff speed, where this is undesirable. This condition could cause a turbulent airflow in the area near to the operating table, where this would possibly induce a light and tiny particle quickly released from the staff.

Figures 8 (*a*) – (*f*) show the airflow velocity distributions inside the OR when a staff was marching towards the operating table at a rate of 1.5 m/s along the z-axis under various ACH values. It was found that the patterns of the air velocity are pretty similar to the previous two cases, where a higher air velocity field has developed adjacent to the moving body. However, the magnitude is greater than the previous cases, since the ACH value of the OR has also increased. It can be observed through Figures 6 to 8 that

the magnitude of air velocity near to the staff's body increases steadily over the range of ACH values and the staff speed by 57 %. However, when the speed of the person walking towards the operating table unchanged, the variation of the ACH values has no significant effect on the airflow velocity distributions. The higher air velocity field near to the human body progressing towards the operating table would cause small and light particles to be released from the person, and this could contaminate the surgical area. A swirling flow pattern can also be seen in the region near to the head.

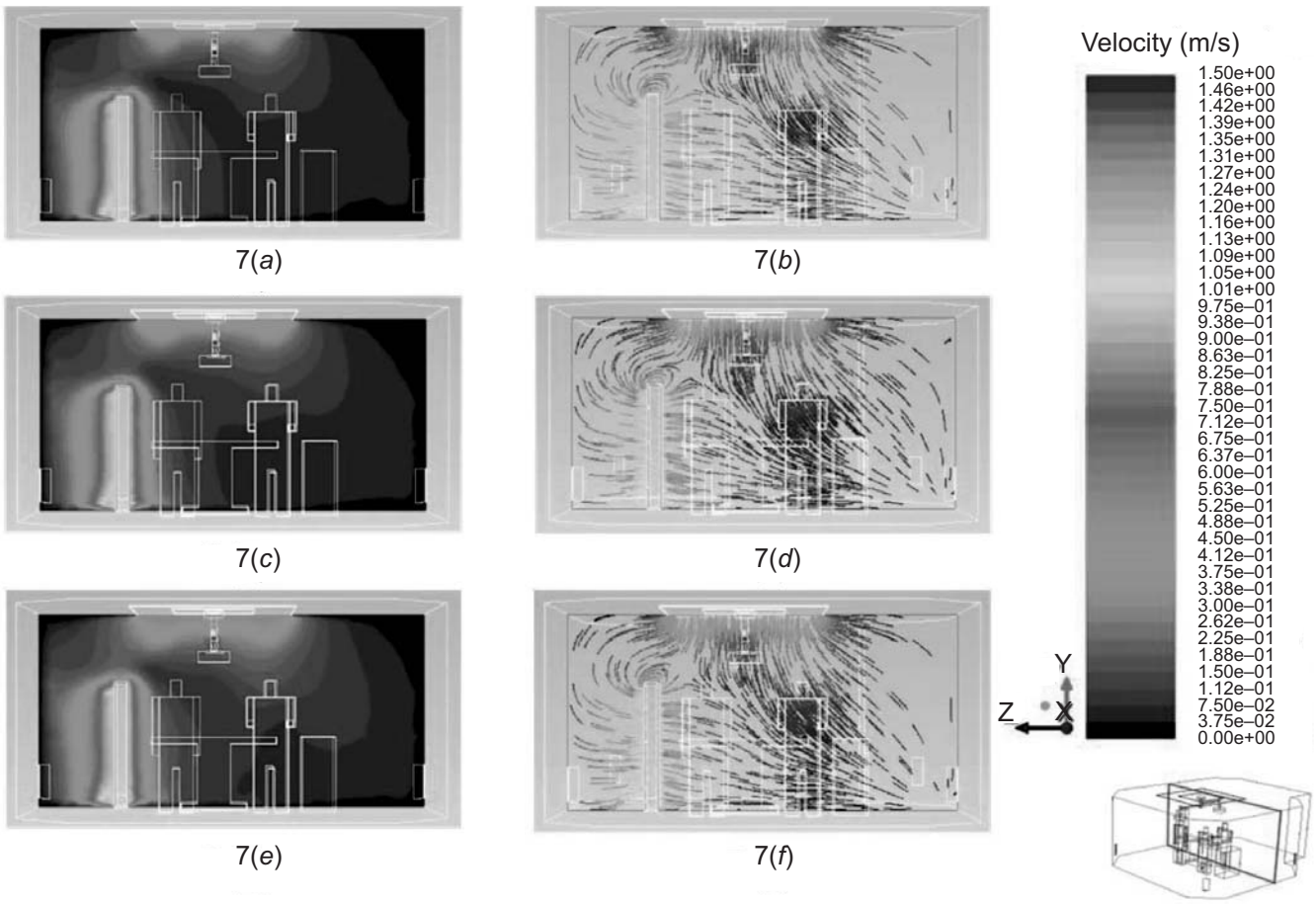

Figure 7: Airflow velocity distributions when a staff travels at a rate of 1.0 m/s under various ACH values of (*a* & *b*) 41/h, (*c* & *d*) 52/h, (*e* & *f*) 63/h

Figure 9 shows the airflow patterns inside the OR when the ACH value was at 63/h under various moving staff speeds towards a surgical table along the z-axis. It was found that when the rate of the moving person increases, it leads to the increment of the airflow velocity in the vicinity of the body as compared to the other regions. For a given ACH value, the air velocity field near to the human's body rises steadily over the range of the staff speeds by 70 %. A swirling flow pattern can also be seen in the area near to the head.

4. CONCLUSION

A computational fluid dynamic method was used to carry out simulations to predict the airflow distribution in a hospital operating room. The goal is to examine the effects of moving rates of a surgical staff and ACH values on the airflow distribution. Results show that under the present ventilation system, the interference of the moving person into the air stream had developed a higher air velocity region in the vicinity of the body as compared to the other regions. For a given staff speed, the magnitude of the airflow near to the staff body increases steadily over the range of ACH values by 57%. While for a given ACH value, the magnitude of the airflow near to the staff body rises steadily over the range the staff speeds by 70%. However, when the speed of the person walking towards the operating table unchanged, the variation of the ACH values has no significant effect on the airflow velocity distributions. The higher air velocity field

near the human body progressing towards the operating table would cause small and light particles to be released from the person, and this could contaminate the surgical area.

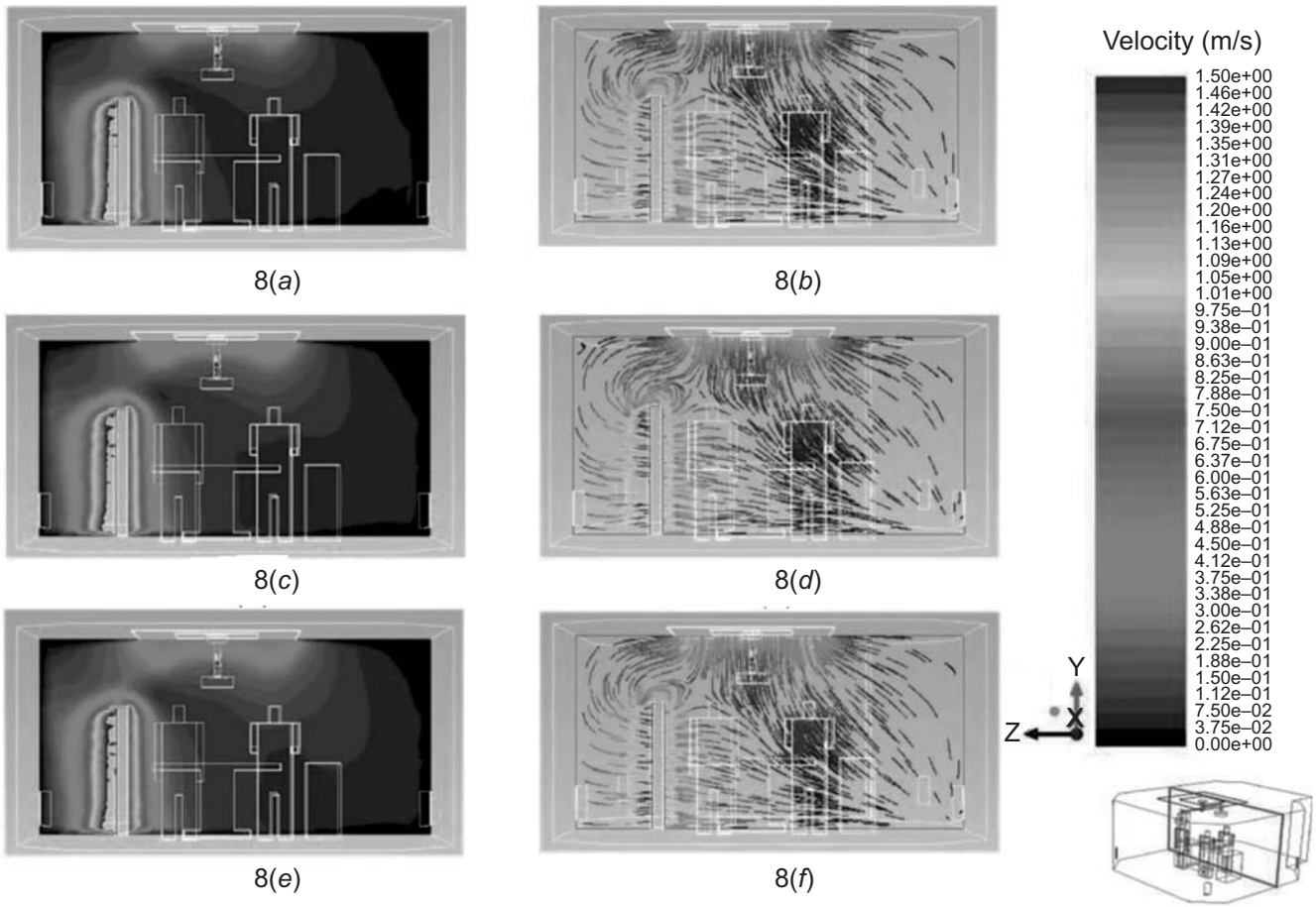

Figure 8: Airflow velocity distributions when a staff travels at a rate of 1.5 m/s under various ACH values of (*a* & *b*) 41/h, (*c* & *d*) 52/h, (*e* & *f*) 63/h

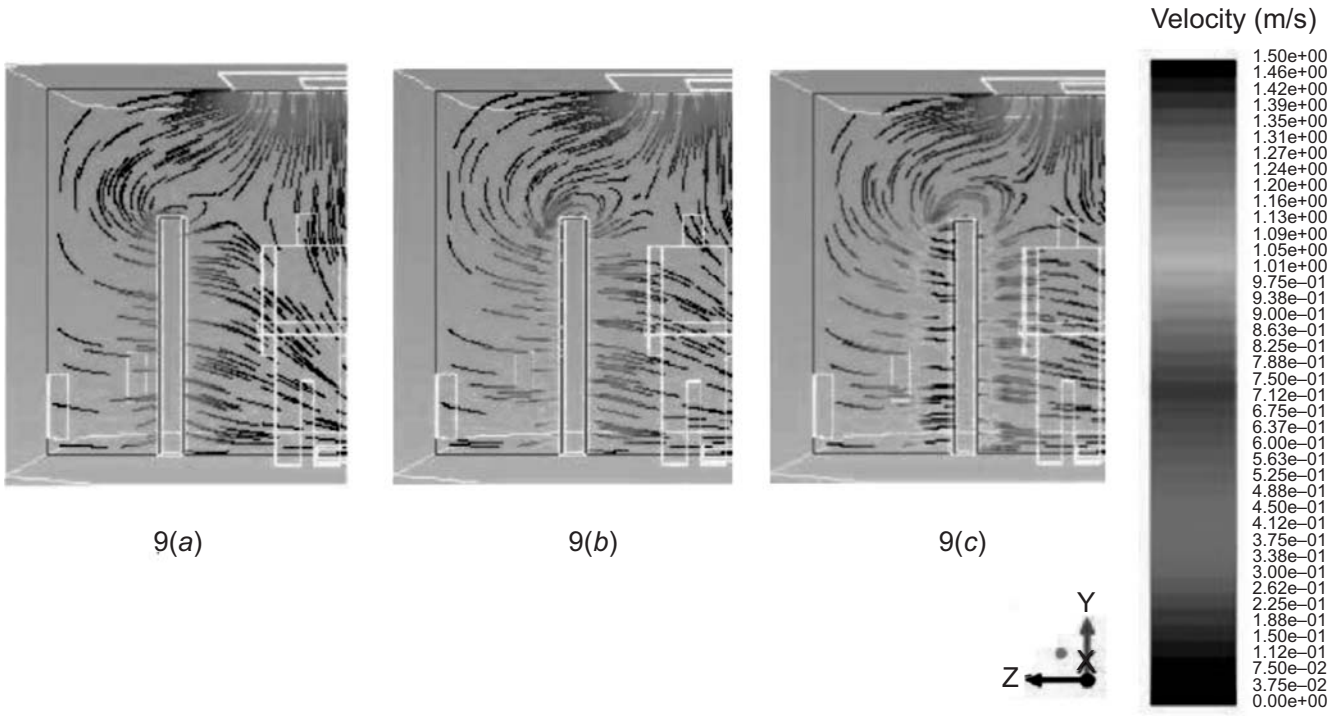

Figurre 9: Path lines illustrations at a velocity of (*a*) 0.5 m/s, (*b*) 1.0 m/s and (*c*) 1.5 m/s

5. ACKNOWLEDGEMENT

The authors would like to acknowledge the supports and funding provided by Universiti Teknologi Malaysia, under the Research University Grant and Ainuddin Wahid Scholarship with Vote No. 14H64 andA.J200000.5900.06000, respectively. The authors are grateful to the staffs of Columbia Asia Hospital, Puchong, Selangor for providing the operating room to facilitate this study.

6. REFERENCES

1. Van Gaever, R., Jacobs, V. A., Diltoer, M., Peeters, L. and Vanlanduit, S. Thermal comfort of the surgical staff in the operating room.*Building and Environment*. 2014. 81: 37-41.
2. Karlatti, S. and Havannavar, I. A comparative prospective study of preoperative antibiotic prophylaxis in the prevention of surgical site infections.*International Surgery Journal*. 2016. 3(1): 141-145.
3. Singh, R., Singla, P. and Chaudhary, U. Surgical site infections: Classification, risk factors, pathogenesis and preventive management.*Int. J. Pharm. Res. Health Sci*. 2014. 2(3): 203-214.
4. Olsen, M. A., Nickel, K. B., Margenthaler, J. A., Fox, I. K., Ball, K. E., Mines, D., Wallace, A. E., Colditz, G. A. and Fraser, V. J. Development of a Risk Prediction Model to Individualize Risk Factors for Surgical Site Infection After Mastectomy.*Annals of surgical oncology*. 2016: 1-9.
5. Birgand, G., Toupet, G., Rukly, S., Antoniotti, G., Deschamps, M.-N., Lepelletier, D., Pornet, C., Stern, J. B., Vandamme, Y.-M. and van der Mee-Marquet, N. Air contamination for predicting wound contamination in clean surgery: A large multicenter study.*American journal of infection control*. 2015. 43(5): 516-521.
6. Mangram, A. J., Horan, T. C., Pearson, M. L., Silver, L. C., Jarvis, W. R. and Committee, H. I. C. P. A. Guideline for prevention of surgical site infection.*American journal of infection control*. 1999. 27(2): 97-134.
7. Anderson, D. J., Podgorny, K., Berríos-Torres, S. I., Bratzler, D. W., Dellinger, E. P., Greene, L., Nyquist, A.-C., Saiman, L., Yokoe, D. S. and Maragakis, L. L. Strategies to prevent surgical site infections in acute care hospitals: 2014 update.*Infection Control & Hospital Epidemiology*. 2014. 35(06): 605-627.
8. Chow, T.-T. and Wang, J. Dynamic simulation on impact of surgeon bending movement on bacteria-carrying particles distribution in operating theatre.*Building and Environment*. 2012. 57: 68-80.
9. Magill, S. S., Hellinger, W., Cohen, J., Kay, R., Bailey, C., Boland, B., Carey, D., de Guzman, J., Dominguez, K. and Edwards, J. Prevalence of healthcare-associated infections in acute care hospitals in Jacksonville, Florida.*Infection Control & Hospital Epidemiology*. 2012. 33(03): 283-291.
10. Ata, A., Lee, J., Bestle, S. L., Desemone, J. and Stain, S. C. Postoperative hyperglycemia and surgical site infection in general surgery patients.*Archives of surgery*. 2010. 145(9): 858-864.
11. Memarzadeh, F. Reducing risks of surgery.*ASHRAE journal*. 2003. 45(2): 28.
12. ASHRAE *Handbook- Applications*. Healthcare Facilities. 1999.
13. Sadrizadeh, S. and Holmberg, S. Effect of a portable ultra-clean exponential airflow unit on the particle distribution in an operating room.*Particuology*. 2015. 18: 170-178.
14. Memarzadeh, F. and Xu, W. Role of air changes per hour (ACH) in possible transmission of airborne infections. Proceedings of the *Building Simulation*: Springer. 15-28.
15. Li, H., Zou, Z. J. and Wang, F. The Effect of Air Change Rate and Cleanroom Garment on Cleanliness in Grade B Cleanroom. Proceedings of the *Applied Mechanics and Materials*: Trans Tech Publ. 514-517.
16. Pereira, M. L., Vilain, R., Galvão, F. H. F., Tribess, A. and Morawska, L. Experimental and Numerical Analysis of the Relationship Between Indoor and Outdoor Airborne Particles in an Operating Room.*Indoor and Built Environment*. 2013. 22(6): 864-875.
17. Shih, Y.-C., Chiu, C.-C. and Wang, O. Dynamic airflow simulation within an isolation room.*Building and environment*. 2007. 42(9): 3194-3209.
18. Standard, I. E. S. T. *IEST-RP-CC006.2*. 1997.
19. Zhai, Z. J. and Osborne, A. L. Simulation-based feasibility study of improved air conditioning systems for hospital operating room.*Frontiers of Architectural Research*. 2013. 2(4): 468-475.
20. Standard, A. S. H. R. A. E. Standard 170 - 2008.*Ventilation of Health Care Facilities*. 2008.

21. Sadrizadeh, S. and Holmberg, S. Surgical clothing systems in laminar airflow operating room: a numerical assessment. *Journal of infection and public health*. 2014. 7(6): 508-516.

22. Wang, J. and Chow, T.-T. Influence of human movement on the transport of airborne infectious particles in hospital. *Journal of Building Performance Simulation*. 2015. 8(4): 205-215.

23. Romano, F., Marocco, L., Gustén, J. and Joppolo, C. M. Numerical and experimental analysis of airborne particles control in an operating theater.*Building and Environment*. 2015. 89: 369-379.

24. Sadrizadeh, S., Holmberg, S. and Nielsen, P. V. Three distinct surgical clothing systems in a turbulent mixing operating room equipped with mobile ultraclean laminar airflow screen: A numerical evaluation.*Science and Technology for the Built Environment*. 2016. 22(3): 337-345.

25. Yao, Z., Zhang, X., Yang, C. and He, F. Flow Characteristics and Turbulence Simulation for an Aircraft Cabin Environment.*Procedia Engineering*. 2015. 121: 1266-1273.

26. Kang, Z., Zhang, Y., Fan, H. and Feng, G. Numerical Simulation of Coughed Droplets in the Air-Conditioning Room. *Procedia Engineering*. 2015. 121: 114-121.

27. Perén, J., van Hooff, T., Leite, B. and Blocken, B. CFD analysis of cross-ventilation of a generic isolated building with asymmetric opening positions: impact of roof angle and opening location.*Building and Environment*. 2015. 85: 263-276.

28. Yau, Y. and Ding, L. A case study on the air distribution in an operating room at Sarawak General Hospital Heart Centre (SGHHC) in Malaysia.*Indoor and Built Environment*. 2014. 23(8): 1129-1141.

29. Fluent, A. Ansys fluent 12.0 users guide.*Ansys Inc*. 2009.

30. Fluent, A. Ansys Fluent 12.0 Theory Guide.*Fluent Inc., Lebanon, NH*. 2009.

31. Standard, A. C. Ashrae handbook: fundamentals. ASHRAE. 2013.

32. S. Aneeka and Z. W. Zhong, "NO_X and CO_2 emissions from current air traffic in ASEAN region and benefits of free route airspace implementation," *Journal of Applied and Physical Sciences,* vol. 2, no. 2. pp. 32-36, 2016.